

## Validation of Multiple Inferior Alveolar Canal Tracing Protocols Based on DICOM Files Generated from Cone Beam Computed Tomography and Multi-Slice Computed Tomography

*Ali Fahd<sup>1</sup>, Ahmed Talaat Temerek<sup>2</sup>, Mohamed T. Ellabban<sup>3</sup>, Mohamed Ahmed Mohamed Ashour<sup>4</sup>, Abeer Madkour Mahmoud<sup>5</sup>, Sarah Mohammed Kenawy<sup>6</sup>*

**Aim:** To evaluate and compare six protocols proposed for inferior alveolar canal tracing on DICOM files generated from different three-dimensional X-ray-based radiographic machines using a mutual third-party software.

**Materials and Methods:** Five adult dry mandibles were scanned three times; one was with a CBCT machine (Planmeca ProMax), and the others were with two different MSCT machines (GE Optima and Philips Brilliance). Imaging data were exported in DICOM format and imported to a third-party software. Then, on each scan, the inferior alveolar canal was traced using six protocols by three independent experienced blinded operators with different specialties. The proposed 540 color-coded traced inferior alveolar canals were compared with a gold standard created by experienced operators from radiology and anatomy departments. The comparison was done using a specially designed 6-point scoring system.

**Results:** The cross-sectional and the hybrid protocols showed the highest significant scores with no significant difference between them regarding all the operators and all machines. The sliced panorama-like protocol could give reliable results, except at the mental foramen where it was user-dependent. The fully automatic protocol failed in inferior alveolar canal tracing in all cases by all operators on all different scans. Operators preferred the CBCT machine, although it did not significantly affect the results.

**Conclusion:** The cross-sectional and the hybrid protocols are the recommended protocols to trace the inferior alveolar canal for giving consistent results among different users and different used machines.

**Keywords:** Mandibular canal, Mandibular nerve, Cone-Beam Computed Tomography, Third party software, Artificial intelligence

1. Associate Professor of Oral and Maxillofacial Radiology, Faculty of Oral and Dental Medicine, Egyptian Russian University, Cairo, Egypt.
  2. Professor, Head of Oral and Maxillofacial Surgery Department, Faculty of Oral and Dental Medicine, South Valley University, Qena, Egypt.
  3. Lecturer of Orthodontics and Dentofacial Orthopedics, Faculty of Dentistry, Assiut University, Assiut, Egypt.
  4. Consultant Radiodiagnosis, Private Center, Qena, Egypt.
  5. Lecturer of Human Anatomy and Embryology, Faculty of Medicine, South Valley University, Qena, Egypt.
  6. Associate Professor of Oral and Maxillofacial Radiology, Faculty of Dentistry, Cairo University, Cairo, Egypt.
- Corresponding author: Ali Fahd, email: dr.ali.fahd.dentist@gmail.com.

## Introduction

The inferior alveolar nerve or the mandibular nerve is the last branch of the trigeminal nerve and is responsible for providing sensory innervation to the regions that correspond to the mandible.<sup>1</sup> The mandibular nerve descends through the mandibular foramen inside the inferior alveolar canal (IAC) until it reaches the mental foramen where it exits and becomes the mental nerve that innervates the chin and lower lip.<sup>1,2</sup> IAC path may vary due to many factors, such as the different mandible shapes and conditions which could cause the mandibular canal to be located at different positions in the jawbone itself.<sup>2,3</sup>

In different surgical procedures, awareness of the IAC path is vital because damaging its content as the mandibular nerves is a cause for loss of sensation in the supplied areas.<sup>4</sup> It is imperative to perform procedures such as dental implants and impaction removal without nerve damage.<sup>1</sup> To perform these surgical procedures safely and with minimal complications, identification of the canal location and any associated variants should be performed pre-operatively through the appropriate advanced three-dimensional (3D) radiographic modality.<sup>5,6</sup>

Considering that multi-slice computed tomography (MSCT) represented a fundamental evolutionary step in the development of advanced radiographic imaging modalities where it offers accurate thorough radiographic imaging owing to its high contrast-to-noise ratio without being obscured by other anatomical structures in different planes along with 3D imaging.<sup>7-9</sup> The MSCT permits imaging, localization, and assessment of mandibular anatomical structures including the IAC.<sup>8,10</sup> In dental procedures, limitations to the routine use of CT imaging may include high doses of radiation exposure, limited access, and high cost.<sup>11</sup>

On the other hand, cone beam computed tomography (CBCT) is a dentist-customized technology that has become a significant oral and maxillofacial radiographic osseous imaging modality providing excellent image quality and diagnostic accuracy.<sup>8,12,13</sup> Therefore, the use of CBCT for oral and maxillofacial procedures became feasible and stands out as an alternative to MSCT.<sup>8,14</sup>

Since X-ray-based imaging depends on the bone condition which sometimes creates a challenge in the detection of the IAC for being not well-corticated or surrounded by confusing marrow spaces, there is a pressing need for evaluating alternative protocols that can help through this dilemma.<sup>5,15</sup> In the same context, there were flaws in some commonly used IAC tracing protocols either due to the challenging bone status, technique sensitivity, or due to anatomical considerations.<sup>5</sup> Therefore, this study aimed to evaluate different protocols proposed for IAC tracing on DICOM files generated from different 3D radiographic X-ray machines (MSCT and CBCT).

## Materials and Methods

This study was conducted on five adult dry human mandibles of undetermined gender obtained from the Department of Human Anatomy and Embryology. The study protocol was approved by the institutional ethical committee, Faculty of Medicine, South Valley University (Code: SVU-FODM-OMS-4-23-5-655).

Adult dry mandibles that were intact from the mandibular foramen distally (posteriorly) to the mental foramen mesially (anteriorly) of at least one side were selected and included in this study. Mandibles with any lesions or impactions at the IAC path were excluded. A simple radiographic stent with gutta-percha markers was fabricated for each mandible. All dry mandibles that matched the inclusion criteria were imaged

by three different 3D imaging machines (one CBCT machine “Planmeca ProMax 3D, Finland” and two MSCT machines “GE Optima 520, USA – Philips Brilliance, Netherlands”). DICOM files were imported to Blue Sky Plan 4.12 software (Blue Sky Bio, Grayslake, IL). The implant planning and surgical guides module was used. After uploading the DICOM dataset, the maximum quality was chosen in the subsampling option.

Regarding CT DICOM files, the dataset was aligned in the correct orientation by using the blue rotational circle then the region of interest (ROI) was cropped or segmented from other data through the movement of the yellow frames (Figure 1). Regarding the CBCT DICOM files, the same protocol was applied for just fine-tuning as correction of the occlusal plane or removing unnecessary extensions (Figure 1). The panoramic curve was customized according to the case (Figure 2). The pre-alignment, the selection of the ROI, panoramic curve customization, and gold standard creation were performed by operators not involved in applying the proposed IAC tracing protocols nor the post-tracing assessment. Then, the project was randomly numbered and saved for another three different independent blinded operators who used the protocols. The baseline gold standard (green color-coded traced inferior alveolar canal) was reached by agreement between two experienced (more than 10 years) operators from the anatomy and radiology departments. They did so after the other three involved operators finished their work.

The three blinded operators (surgeon, orthodontist, and radiologist) with more than 10 years of experience performed six different IAC tracing protocols with different color coding for each method. Each operator applied the protocols for each case and repeated the full sequences on every imaging scan. They started with the automatic

protocol followed by image modification and enhancement followed by applying the other semiautomatic or manual protocols. The image display parameters in terms of contrast and density were enhanced based on the radiographic stent, the gutta-percha markers, and the bone and teeth at the area of the mental foramen (until all were shown clearly) (Figure 2).

The traced IAC was hidden by the operator before tracing the canal again by the next protocol. The protocols were adopted from the study of Fahd et al<sup>5</sup> but with modifications such as adding a fully automatic protocol (the new auto-detect protocol) without any operator intervention. Also changing the name of the automatic canal tracing protocol of their study into the detect protocol in our study was done to avoid confusion. The following is a full description of the applied protocols (Figures 2-5):

**Protocol 1** or the **autodetect** protocol (fully automated protocol) (orange color-coded) was done by just clicking the autodetect nerves tool in the nerve panel tools (Figure 2) and waiting for the software to draw the IAC (fully automatic or artificial intelligence-based protocol). This protocol was applied before any manual adjustment of the images.

**Protocol 2** or the **detect** protocol (red color-coded) was done by activating the detect tool in the nerve panel tools and then clicking at the mental foramen on the corresponding cross-sectional slice (Figure 2). The software automatically traced the rest of the canal (semi-automatic protocol).

**Protocol 3** or the **full-thickness** panorama-like protocol (white color-coded) was done by tracing the IAC on the full-thickness reformatted panorama by pointing 6 to 10 marks on the pathway of the canal between the most distal end (corresponding to the mandibular foramen) to the most mesial end (corresponding to the mental foramen) (Figure 3).

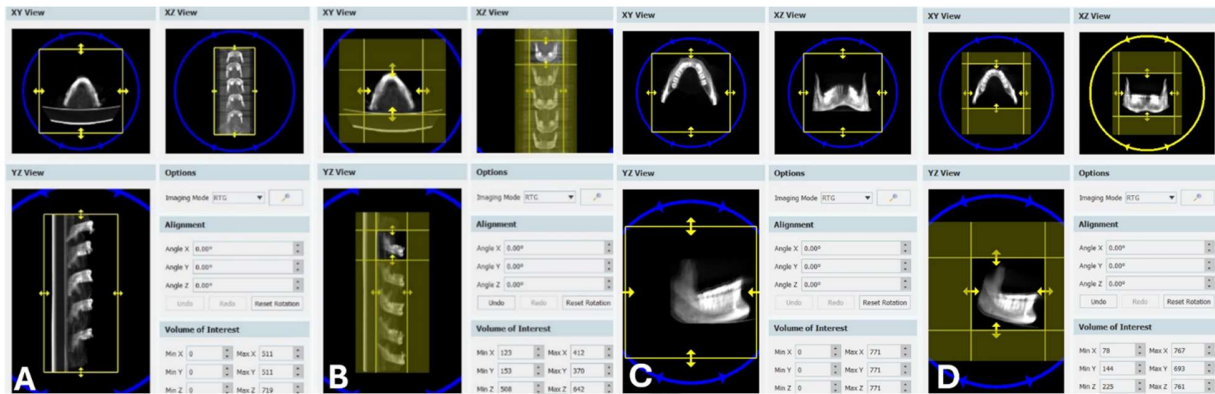


Figure 1: CT ROI (A) before and (B) after alignment and selection. The blue circle is used for rotational movement for proper alignment (should be done before ROI selection by the yellow frame). CBCT ROI orientation and selection before (C) and after (D). Note that the misorientation of the occlusal plane is due to the resting of the inferior border of the mandible on the special base during image acquisition.

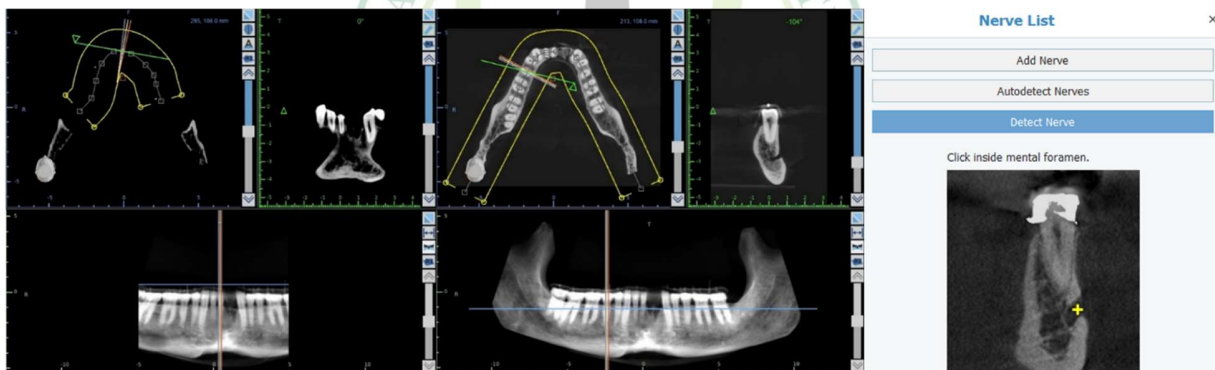


Figure 2: Creating the reformatted panorama-like view and the adjustment of image display parameters based on the stent, the gutta-percha, and the bone and teeth at the mental foramen slice as shown in the 360-degree view (orientation of the 360-degree view is shown by the green reference line at the axial slice). Note the nerve list panel which shows the three available tracing options and how the detect nerve tool works by just making one click at the mental foramen.

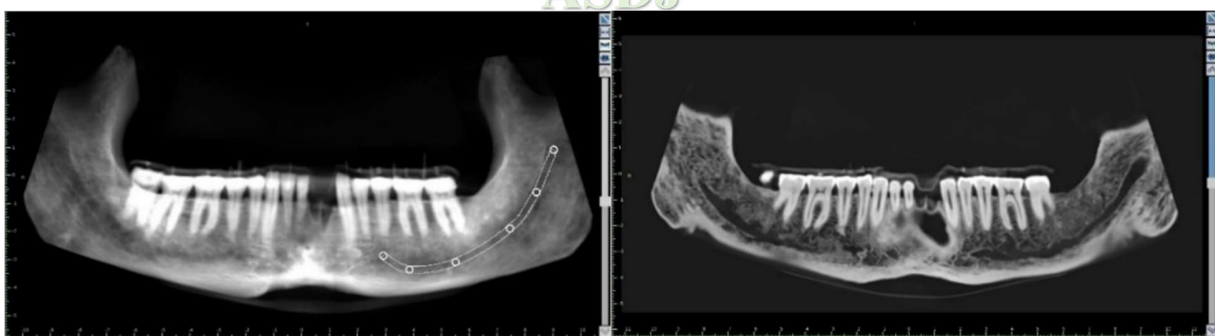


Figure 3: Left: Full-thickness reformatted panorama-like view (composite view) where 6 points were placed. Right: Sliced panorama-like view where the slice was navigated till identification of the IAC. Note how difficult it is to identify mental foramen on both sides and that the right-side canal is not fully shown especially at the starting and ending areas where it requires multiple navigations to be shown and traced.



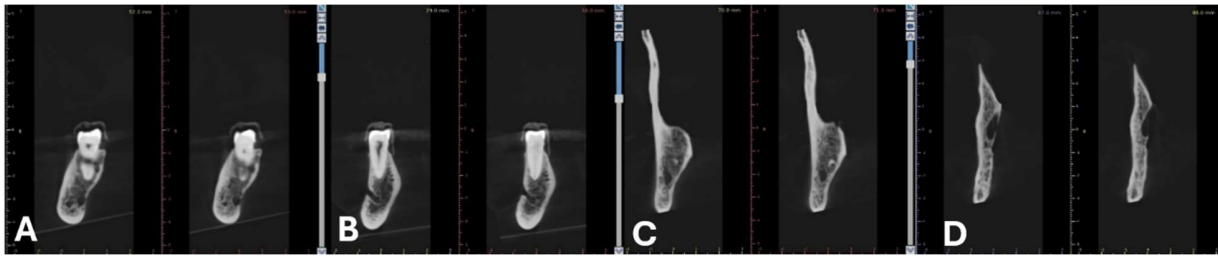


Figure (4): Serial cross-sectional cuts before tracing at different positions. Note the confusing adjacent marrow spaces and bone condition (A) showing the importance of tracing and color coding for identification. Note the clear presentation of the inferior alveolar canal at the selected sites proposed for the hybrid protocol, at the mental foramen (B), the ramus (C), and the mandibular foramen (C).

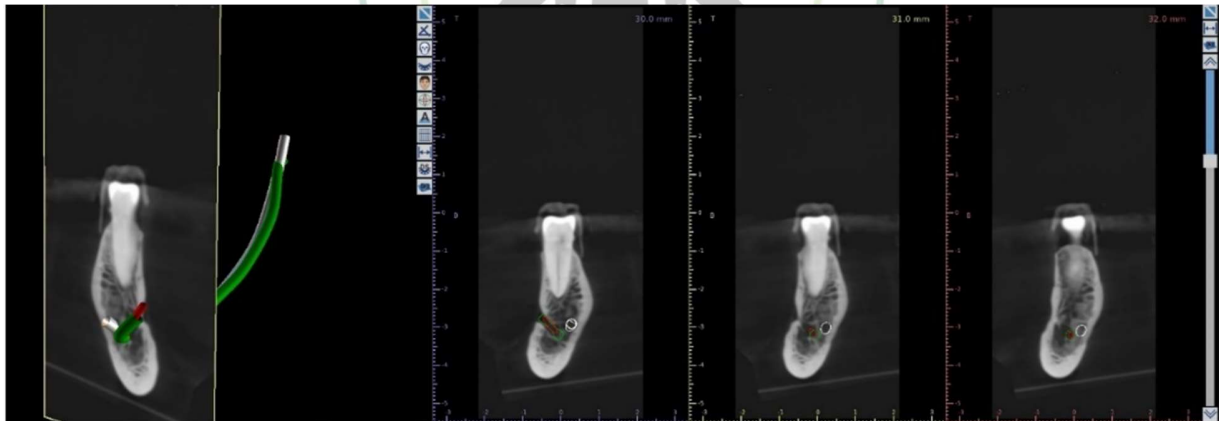


Figure (5): Left: 3D view of three color-coded traced IAC with 2D cross-sectional overly (the mandible was hidden by thresholding) and the adjacent serial cross-sectional slices. Note the failure of the full-thickness panorama-like protocol (white) in buccolingual orientation at the mental foramen and the horizontal mismatching. Note the different diameters of the tracings.

**Protocol 4** or the **sliced** panorama-like protocol (blue color-coded) was done as the previous protocol but on a sliced reformatted panorama where the images were navigated antero-posteriorly until the display of the clear pathway of the IAC to be traced. The operator was allowed to navigate according to the target part of the canal (anatomic location) (Figure 3).

**Protocol 5** or the **cross-sectional** protocol (yellow color-coded) was done by placing points or marks (from 6 to 10) on the IAC pathway as shown in the serial cross-sectional cuts starting from the mental foramen to the mandibular foramen (Figure 4).

**Protocol 6** or the **hybrid** protocol (brown color-coded) was done by pointing the marks on different images where anatomic IAC locations at or near the mandibular foramen and the mental foramen were traced on cross-sectional cuts and the rest of the IAC path was traced on navigated sliced panorama-like view. The operator was allowed to check and edit points on the 360-degree rotational view (Figures 3 and 4).

Another non-previously involved blinded experienced oral and maxillofacial radiologist compared the different traced IACs by only showing the gold standard against one of the traced canals under investigation. The verification was performed on all views including the 3D volume rendering view (Figure 5).

The comparison was based on six criteria or a created 6-point scoring system where a score of 1 was given every time the traced IACs were matched and zero when the traced IACs were apart. Suppose the traced canal showed mild deviation (as defined by following the gold standard course and the deviation is contained within the canal boundaries). In that case, it is accepted and given a score of one or otherwise a score of zero. The traced canal was not evaluated and considered failed if less than half of the canal

was traced. The scoring points included matching distally (at the mandibular foramen) or matching mesially (at the mental foramen) or IAC course regularity (regular or irregular pathway) or continuity throughout the IAC course (no interruption) or matching horizontally (buccolingual position) or matching vertically (superior and inferior position). Five points of the scoring system were previously described in the study of Fahd et al.<sup>5</sup>

Values were presented as median, mean, standard deviation (SD), and confidence intervals. To evaluate inter-observer agreement, Cronbach's reliability coefficient test was used (the closer Cronbach's  $\alpha$  coefficient is to 1.0, the higher the reliability and vice versa). Data were explored for normality using the Kolmogorov-Smirnov test of normality. Kruskal Wallis, Mann-Whitney, ANOVA, and Post hoc tests were proposed for comparisons according to data type. The significance level was set at  $p \leq 0.05$ . Statistical analysis was performed using a commercially available software program (SPSS 18.0-Statistical Package for Scientific Studies, SPSS, Inc., Chicago, IL, USA) for Windows.

## Results

A total of 450 IAC tracings were done as the automatic detection tracing protocol failed to produce any IAC with all the observers in all imaging modalities. Each operator succeeded in manually tracing all the IACs using the different protocols on the DICOM files generated from the different machines. Regarding the inter-observer agreement, Cronbach's reliability coefficient test revealed a very good inter-observer agreement regarding all measurements conducted in the present study (0.898, with a

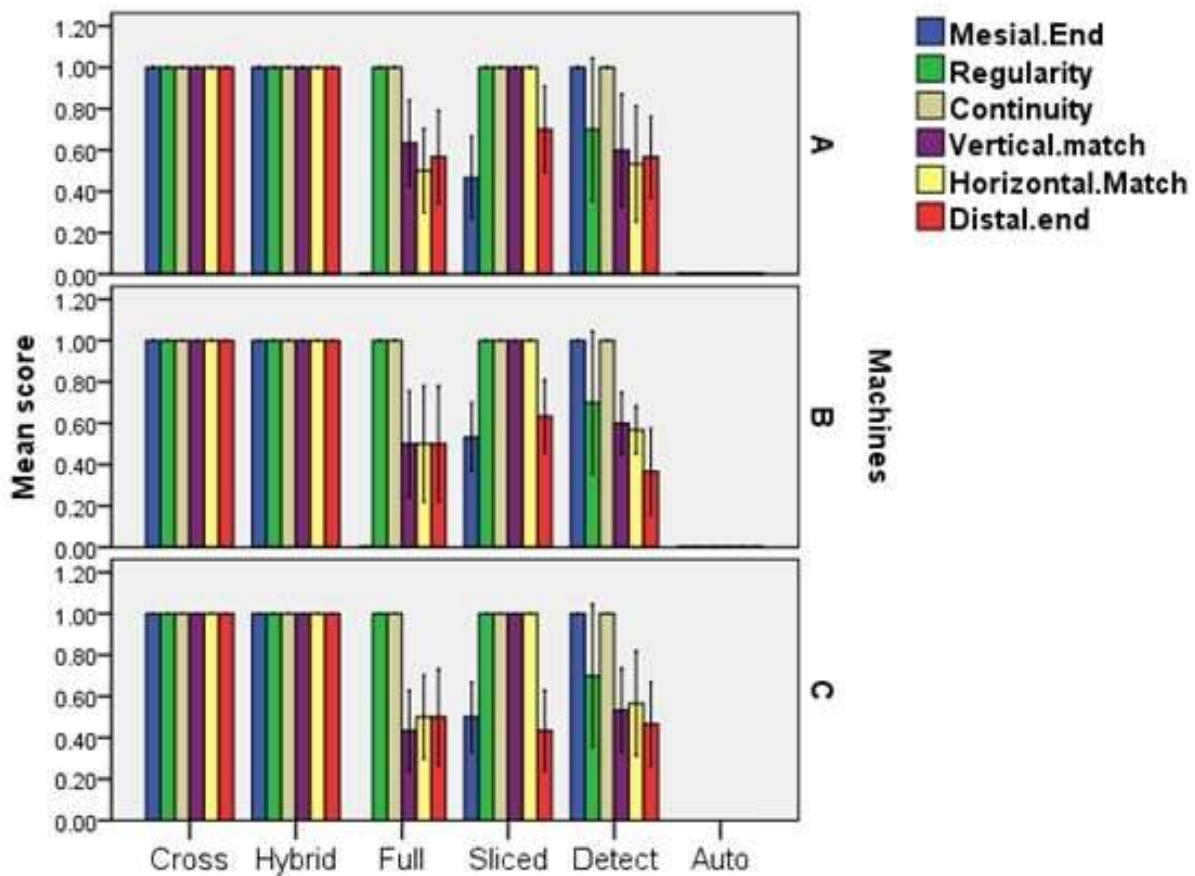


Figure (6): Bar chart illustrating the mean score for each item. A) Planmeca CBCT machine. B) Philips Brilliance MSCT machine. C) GE Optima MSCT Machine.

confidence interval of 0.887 to 0.908). Therefore, the average of the examiners can be used for statistical analysis.

The cross-sectional and the hybrid protocols showed the highest significant scores with no significant difference between them, and these results were the same regarding all the operators and all 3D machines' scans. The sliced panorama-like protocol showed a significantly lesser score than the cross-sectional and the hybrid protocols but still significantly higher than the other three protocols. The full-thickness panorama-like and the detect protocols showed a significantly lesser score than the cross-sectional, the hybrid, and the sliced

panorama-like protocols. The automatic protocol showed no results (failure) in all cases by all operators on all machines' scans. Figure (6) represents the summary of the results. The operators blindly agreed on the ease of manipulation of the DICOM files generated from the CBCT machine and they also stated the operator dependence sliced panorama-like protocol at the mental foramen.

Regardless of the technique, the Planmeca CBCT machine recorded the highest total score ( $4.21 \pm 2.14$ ), followed by the Philips Brilliance MSCT machine ( $4.15 \pm 2.12$ ), with the lowest value recorded in the GE Optima MSCT Machine

(4.11±2.11). The difference between machines didn't reach the level of statistical significance ( $p=0.48$ ). Regardless of the machine, statistically significant higher total scores were recorded using the cross-sectional and hybrid protocols (6±0), followed by the sliced panorama-like (5.09±0.38), then the detect protocol (4.3±0.89), then the full-thickness panorama-like protocol (3.54±.62), with a significantly lower value in the autodetect protocol (0±0). The difference between techniques was statistically significant ( $p=0.000$ ) except for the cross-sectional and the hybrid protocols. The interaction of the machines and techniques variables didn't have a statistically significant effect ( $p=0.99$ ).

## Discussion

Radiographically, IAC can be defined as a radiolucent linear nearly horizontal anatomical landmark situated inferior to the lower posterior teeth, which has a well-defined, roughly rounded corticated border.<sup>5</sup> However, various forms, places, and orientations are documented in the literature.<sup>16, 17</sup> If the IAC and its enclosed neurovascular bundle are not appropriately detected and protected, the patients could suffer complications such as hemorrhage and neuropathic manifestations.<sup>18</sup> As a result, an appropriate radiographic approach should be used to identify the canal location before surgery to prevent damaging effects.<sup>6</sup> A major goal of this research was to shield patients from preventable injuries and the consequences that follow, which may lower their quality of life.

As high as 20% of cases, clinicians may encounter a challenge in detecting the IAC, which can be explained by the condition of the surrounding bone and the integrity of the canal cortical boundaries.<sup>15, 19</sup> Therefore, different software manipulation methods are required as alternative solutions for critical cases of difficult IAC tracing. Generally, all

dental clinicians should be aware of a lot of software manipulation protocols and alternatives to be able to handle challenging cases.<sup>20</sup> This was another goal of this research work.

It is not new to search for alternative techniques for IAC tracing; even outside x-ray-based modalities, as Beck et al.<sup>21</sup> who assessed the reliability of magnetic resonance imaging (MRI) in detecting the IAC and its relation to the third molars. Sorrowfully, many dental professionals are unfamiliar with using MRI despite its merits such as the high soft tissue resolution and the absence of ionizing radiation. This unfamiliarity affected their results as evidenced by the lower levels of intra- and inter-observer agreement<sup>21</sup>, unlike this study which showed high agreement that may be explained by the operator-friendly techniques and software.

Considering that, the radiological assessment of IAC is the concern of several studies aiming at defining its normal course, and detecting its anatomical variations, to avoid the injury of the neurovascular bundle during dental and oral surgical procedures.<sup>22, 23</sup> Researchers' methods for accurately mapping the IAC vary depending on the imaging modality, the selected software, and the applied protocol.<sup>5</sup> Our study assessed different imaging modalities and software manipulation protocols, which was a respectable point to address. MSCT is sometimes preferred by maxillofacial surgeons<sup>24</sup> while CBCT is usually the choice of other dental specialists<sup>15</sup>, this study applied the protocols to both imaging modalities.

Using different machines for the same protocol was essential to study the effect of changing the 3D imaging modality on the accuracy of the results.<sup>25</sup> Liang et al.<sup>26</sup> showed how variable the image display was between different machines, which may explain why the CBCT machine provided higher results in the hands of the operators



despite of not reaching the significant level. In the same context, knowing how the image display parameters affect the diagnostic accuracy,<sup>20</sup> we used a radiographic stent to standardize the visual characteristics of the images between operators.

In the present study, dry mandibles were used to avoid the hazards of unjustified doses of repeated radiation exposure to patients or volunteers as MSCT and CBCT modalities are associated with increased exposure to ionizing radiation.<sup>27, 28</sup> However, Waltrick et al.<sup>29</sup> work on dry mandibles demonstrated that the IAC in the dry specimens would be more radiolucent and more visible than those in living subjects as they are air-filled and devoid of the neurovascular structures. This could explain why the human-intelligence-based cross-sectional and hybrid protocols in our study showed 100% accuracy in comparison with the gold standard. Also, this may be a factor that should be considered as a cause of failure of the automatic protocols since the artificial intelligence-based detection may require specific visual characteristics of the canal which may depend on its content. It is worth mentioning that the automatic protocol was applied before any manual adjustment of the images to judge the fully automatic functionality of the tool without any operator intervention which may be another cause of failure.

On the other hand, another crucial limitation to address for this study was the small sample size. Dry mandibles require special ethical clearance and are not easily available.<sup>5</sup> This study protocol was preapproved by the institutional ethical committee. All the dry mandibles that matched the eligibility criteria were used in the study. Fortunately, the statistical analysis revealed statistically significant results.

Five points of the scoring system used for evaluation and comparison were previously described in the study of Fahd et

al.<sup>5</sup> In this study, a new point was added which was the continuity of the traced IAC because the artificial intelligence-based IAC tracing was expected to be interrupted in areas of narrowing of the IAC at certain anatomical positions. Further studies are recommended to be done using retrospective real patient data and with different artificial intelligence-based software to overcome the limitations of this study and to test the hypothesis of needing a score based on the continuity of the traced IAC. Expecting the points where artificial intelligence fails is very important for any evaluating scoring system.

A virtual nerve tracing tool provided by various dental DICOM viewing software is helpful in IAC detection by enabling the users to mark sites on certain slices with distinct IAC anatomy, even at slightly separated locations. These points are then automatically linked into a single virtual canal color mapping.<sup>30, 31</sup> In this study, the Blue Sky Plan software was used as a third-party software that can handle DICOM files generated from both CBCT and MSCT machines so the same software could be used for all datasets. Also, the surgical guide module was the choice for the advantage of enabling prework alignment and selection of the ROI.

The high score of the cross-sectional protocol was expected for being a precise, and user-friendly method of canal tracing, which favors it for many clinicians.<sup>32</sup> This study proved that this protocol's reliability was high and consistent between different observers and different imaging modalities. The main benefit was the accurate marking of the IAC at mental foramen as its orientation in the buccolingual dimension was favorable on the cross-sectional cuts.

For accurate canal tracing, the exact IAC anatomy must be located and marked. This explains why tracing on a full-thickness reformatted panorama was unable to provide

an accurate horizontal location of the canal because the software erroneously inserts the surface-done marks automatically inside the bone in any layer of the multiple composite layers (maybe 25 different options of layers). This explained why the sliced panorama-like protocol was more accurate as the operators could navigate through the path of the IAC and place the marks in a small slice thickness, so the software had no chance for errors. The combined advantages of the sliced reformatted panorama-like in simple reliable canal path recognition and the cross-sectional protocol in simple reliable detection of buccolingual directed paths (as mental foramen) were integrated into the hybrid protocols which explained its high accuracy results.

### Conclusion

The cross-sectional and hybrid protocols for IAC tracing are the most recommended protocols for giving consistent results among different users and with different imaging machines. The hybrid protocol is recommended to be used in cases where there are confusing adjacent marrow spaces or challenging bone conditions leading to difficulty in tracing in cross-sectional cuts. Additionally, the sliced panorama-like protocol can give a reliable result but is user-dependent in tracing at mental foramen. However, the full-thickness-panorama-like and the detect protocols are not recommended. Unfortunately, the automatic protocol showed failure with all users, but an in vivo study is recommended as the results may be related to the type of study. Finally, clinicians should be trained on different software manipulation protocols to be able to deal with challenging cases.

### Funding

None.

### Data availability

Part of the data is available from the corresponding author upon reasonable request.

### Declarations

The authors declare no competing interests.

### Ethical approval

The study protocol was approved by the institutional ethical committee (Code: SVU-FODM-OMS-4-23-5-655).

### References

1. Nguyen JD, Duong H. Anatomy, Head and Neck: Alveolar Nerve. StatPearls: StatPearls Publishing; 2024.
2. Stein P, Brueckner J, Milliner M. Sensory innervation of mandibular teeth by the nerve to the mylohyoid: implications in local anesthesia. Clin Anat 2007;20:591-5.
3. Wolf KT, Brokaw EJ, Bell A, Joy A. Variant Inferior Alveolar Nerves and Implications for Local Anesthesia. Anesth Prog 2016;63:84-90.
4. Kang F, Sah MK, Fei G. Determining the risk relationship associated with inferior alveolar nerve injury following removal of mandibular third molar teeth: A systematic review. J Stomatol Oral Maxillofac Surg 2020;121:63-9.
5. Fahd A, Temerek AT, Kenawy SM. Validation of different protocols of inferior alveolar canal tracing using cone beam computed tomography (CBCT). Dento maxillo facial radiology 2022;51:20220016.
6. Friedland B, Donoff B, Dodson TB. The use of 3-dimensional reconstructions to evaluate the anatomic relationship of the mandibular canal and impacted mandibular third molars. J Oral Maxillofac Surg 2008;66:1678-85.
7. Hofmann E, Medelnik J, Fink M, Lell M, Hirschfelder U. Three-dimensional volume tomographic study of the imaging accuracy of impacted teeth: MSCT and CBCT comparison--an in vitro study. Eur J Orthod 2013;35:286-94.
8. Gaia BF, Sales MA, Perrella A, Fenyó-Pereira M, Cavalcanti MG. Comparison between cone-beam and multislice computed tomography for identification of simulated bone lesions. Braz Oral Res 2011;25:362-8.
9. Nicolielo LFP, Van Dessel J, Shaheen E, Letelier C, Codari M, Politis C, et al. Validation of a novel imaging approach using multi-slice CT and cone-beam CT to follow-up on condylar remodeling after bimaxillary surgery. Int J Oral Sci 2017;9:139-44.
10. Rashesuren O, Choi JW, Han WJ, Kim EK. Assessment of bifid and trifid mandibular canals using

cone-beam computed tomography. *Imaging science in dentistry* 2014;44:229-36.

11. Loubele M, Guerrero ME, Jacobs R, Suetens P, van Steenberghe D. A comparison of jaw dimensional and quality assessments of bone characteristics with cone-beam CT, spiral tomography, and multi-slice spiral CT. *The International journal of oral & maxillofacial implants* 2007;22:446-54.

12. Scarfe WC, Farman AG, Sukovic P. Clinical applications of cone-beam computed tomography in dental practice. *Journal (Canadian Dental Association)* 2006;72:75-80.

13. Fahd A, Abd-El Ghaffar Y, El-Shenawy H, Khalifa M, Dahaba M. Bone Changes in dental implant combined with laser therapy: a split mouth study. *Researcher* 2017;9:68-74.

14. AbdElGhaffar Y, Temerek AT, Hammad HG, Fahd A. Flapless dental implant surgery as a successful patient relevant treatment option: a 5-year retrospective clinical and radiographic evaluation. *Egyptian Dental Journal* 2019;65:197-204.

15. Fahd A, ElBeshlawy D. Cone Beam Computed Tomography and Preoperative Bone Quality Assessment for Dental Implants: Myth and Truth. *ERU Research Journal* 2023;2:541-9.

16. Pria CM, Masood F, Beckerley JM, Carson RE. Study of the inferior alveolar canal and mental foramen on digital panoramic images. *J Contemp Dent Pract* 2011;12:265-71.

17. Fahd A, Temerek AT, Ellabban MT, Adam SAN, Shaheen S, Refai MS, et al. Cone-beam computed tomography-based radiographic considerations in impacted lower third molars: Think outside the box. *Imaging science in dentistry* 2023;53:137-44.

18. Politis C, Lambrichts I, Agbaje JO. Neuropathic pain after orthognathic surgery. *Oral surgery, oral medicine, oral pathology and oral radiology* 2014;117:e102-7.

19. Oliveira-Santos C, Capelozza ALÁ, Dezzoti MSG, Fischer CM, Poleti ML, Rubira-Bullen IRF. Visibility of the mandibular canal on CBCT crosssectional images. *Journal of Applied Oral Science* 2011;19:240-3.

20. Elmesellawy MY, Fahd A, Nasr M. Assessment of Mesiobuccal Root Canal Curvature in Maxillary Molars of Egyptian Population: A Standardized CBCT-Based Radiographic Protocol. *Ain Shams Dental Journal* 2024;34:195-202.

21. Beck F, Austermann S, Bertl K, Ulm C, Lettner S, Toelly A, et al. Is MRI a viable alternative to CT/CBCT to identify the course of the inferior alveolar nerve in relation to the roots of the third molars? *Clinical oral investigations* 2021;25:3861-71.

22. Kensara J, Jayam R, Almanea M, Bin Rubaia'an MA, Alshareef N, Abed H. Radiological assessment of the inferior alveolar canal and mental foramen using

cone beam computed tomography for pre-operative evaluation of surgeries in the mandible: A single-center five-year retrospective study. *The Saudi dental journal* 2024;36:91-8.

23. Yilmaz D, Ataman-Duruel ET, Beycioğlu Z, Goyushov S, Çimen T, Duruel O, et al. The Radiological Evaluation of Mandibular Canal Related Variables in Mandibular Third Molar Region: a Retrospective Multicenter Study. *Journal of oral & maxillofacial research* 2022;13:e2.

24. Gomes LR, Gomes MR, Gonçalves JR, Ruellas AC, Wolford LM, Paniagua B, et al. Cone beam computed tomography-based models versus multislice spiral computed tomography-based models for assessing condylar morphology. *Oral surgery, oral medicine, oral pathology and oral radiology* 2016;121:96-105.

25. Adibi S, Shahidi S, Nikanjam S, Paknahad M, Ranjbar M. Influence of head position on the CBCT accuracy in assessment of the proximity of the root apices to the inferior alveolar canal. *Journal of Dentistry* 2017;18:181.

26. Liang X, Jacobs R, Hassan B, Li L, Pauwels R, Corpas L, et al. A comparative evaluation of Cone Beam Computed Tomography (CBCT) and Multi-Slice CT (MSCT) Part I. On subjective image quality. *European journal of radiology* 2010;75:265-9.

27. Belmans N, Oenning AC, Salmon B, Baselet B, Tabury K, Lucas S, et al. Radiobiological risks following dentomaxillofacial imaging: should we be concerned? *Dento maxillo facial radiology* 2021;50:20210153.

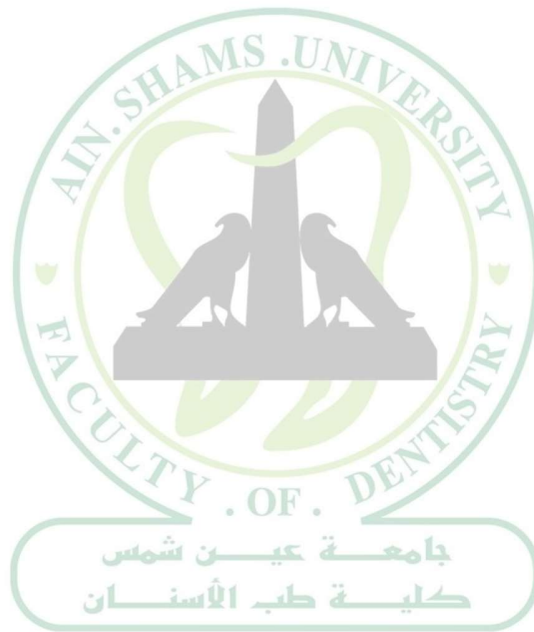
28. Lee CY, Koval TM, Suzuki JB. Low-Dose Radiation Risks of Computerized Tomography and Cone Beam Computerized Tomography: Reducing the Fear and Controversy. *The Journal of oral implantology* 2015;41:e223-30.

29. Waltrick KB, Nunes de Abreu Junior MJ, Corrêa M, Zastrow MD, Dutra VD. Accuracy of linear measurements and visibility of the mandibular canal of cone-beam computed tomography images with different voxel sizes: an in vitro study. *Journal of periodontology* 2013;84:68-77.

30. Agbaje JO, Van de Castele E, Salem AS, Anumendem D, Lambrichts I, Politis C. Tracking of the inferior alveolar nerve: its implication in surgical planning. *Clinical oral investigations* 2017;21:2213-20.

31. Weckx A, Agbaje JO, Sun Y, Jacobs R, Politis C. Visualization techniques of the inferior alveolar nerve (IAN): a narrative review. *Surgical and radiologic anatomy : SRA* 2016;38:55-63.

32. Khorshidi H, Raofi S, Ghapanchi J, Shahidi S, Paknahad M. Cone Beam Computed Tomographic Analysis of the Course and Position of Mandibular Canal. Journal of maxillofacial and oral surgery 2017;16:306-11.



ASDJ

Ain Shams Dental Journal